

# **METAMORPHIC MULTIMODE ANTENNA FOR AMPHIBIOUS MILITARY COMMUNICATIONS USING SPIRAL ANTENNA**

**A PROJECT REPORT**

**[PHASE II]**

*Submitted by*

**DINESH KUMAR A K** **(113222041040)**

**SANTHOSH S** **(113222041137)**

**KALAIVANAN B** **(113222041072)**

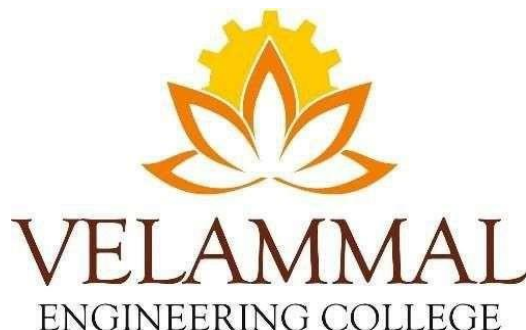
*In partial fulfilment for the award of the degree*

*Of*

**BACHELOR OF ENGINEERING**

**IN**

**ELECTRONICS AND COMMUNICATION ENGINEERING**



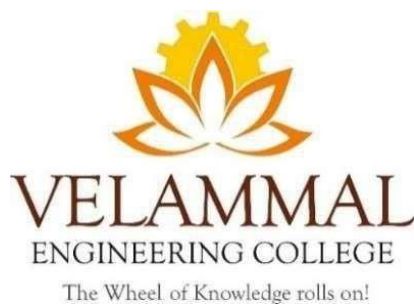
*The Wheel of Knowledge rolls on!*

**VELAMMAL ENGINEERING COLLEGE, CHENNAI-66.**

*(An Autonomous Institution, Affiliated to Anna University, Chennai)*

**OCTOBER 2025**

# **VELAMMAL ENGINEERING COLLEGE, CHENNAI-66.**



## **BONAFIDE CERTIFICATE**

Certified that this project report, "**METAMORPHIC MULTIMODE ANTENNA FOR AMPHIBIOUS MILITARY COMMUNICATIONS USING SPIRAL ANTENNA**" is the Bonafide work of "**DINESH KUMAR A K, SANTHOSH S, KALAIYANAN B**" who carried out the project work under my supervision.

### **Signature**

**Dr. S. MARY JOANS**  
**PROFESSOR &**  
**HEAD OF THE DEPARTMENT**  
Department of Electronics and  
Communication Engineering  
Velammal Engineering College  
Ambattur – Redhills Road  
Chennai-66.

### **Signature**

**Dr.S.MANJU**  
**SUPERVISOR**  
**ASSOCIATE PROFESSOR**  
Department of Electronics and  
Communication Engineering  
Velammal Engineering College  
Ambattur – Redhills Road  
Chennai-66.

# **CERTIFICATE OF EVALUATION**

COLLEGE NAME: VELAMMAL ENGINEERING COLLEGE

BRANCH : ELECTRONICS AND COMMUNICATION ENGINEERING

SEMESTER : VII

<b>Sl. No</b>	<b>Name of the students who has done the project</b>	<b>Title of the project</b>	<b>Name of the supervisor with designation</b>
1	DINESH KUMAR A K	METAMORPHIC MULTIMODE ANTENNA FOR AMPHIBIOUS MILITARY COMMUNICATION USING SPIRAL ANTENNA	Dr.S.MANJU ASSOCIATE PROFESSOR
2	SANTHOSH S		
3	KALAIVANAN B		

This report of project work submitted by the above students in the partial fulfillment for the award of Bachelor of Engineering Degree in Anna University was evaluated and confirmed to be the reports of the work done by the above students and then assessed.

Submitted for Internal Evaluation held on \_\_\_\_\_

**Internal Examiner**

**External Examiner**

## ABSTRACT

This work presents the design and performance analysis of two Archimedean spiral patch antennas developed on an FR4 substrate for high-frequency communication applications. Both antennas are designed within the 12–18 GHz frequency range, focusing on the effect of inter-arm spacing on key performance parameters such as return loss, bandwidth, gain, and directivity. The first spiral configuration, features a smaller gap between spiral arms, resulting in dual-band operation with resonant frequencies at 15 GHz and 17 GHz. It exhibits bandwidths of 700 MHz and 2 GHz, a gain of 8.1 dB, and directivity of 9.78, demonstrating enhanced coupling and broadband characteristics. The second configuration spiral Antenna incorporates a larger arm spacing, leading to a single-band resonance at 14.2 GHz with an excellent return loss of –45 dB, VSWR of 1.1, gain of 5.28 dB, and directivity of 6.92. Comparative analysis using HFSS simulations reveals that decreasing inter-arm spacing increases bandwidth and gain by improving current coupling, while increasing the spacing enhances impedance matching and return loss. Both antennas provide circular polarization and stable radiation patterns, making them suitable for applications such as radar, satellite communication, and ultra-wideband (UWB) systems. The results confirm that geometric tuning of spiral arm spacing can effectively tailor antenna performance for either broadband (dual-band) or narrowband (single-band) operation, offering flexibility in modern high-frequency communication system design.

## **ACKNOWLEDGEMENT**

First of all, we thank God almighty, for guiding and helping us in every stage of our project. It is our pleasant duty to express deep sense of gratitude to our beloved **Chairman, Thiru. M. V. Muthuramalingam** for his support and guidance, which greatly contributed to the successful completion of this project.

We would like to express our heartfelt thanks to our respected **Chief Executive Officer, Thiru. M. V. M. Velmurugan** for his kind encouragement.

We would like to express our heartfelt thanks to our respected **Deputy Chief Executive Officer, Thiru. V. Karthik Muthuramalingam** for his support.

We express our gratitude and thanks to our beloved **Principal, Dr. S. Satish Kumar** for his inspirational support during the course of the project.

We would especially like to thank our **Head of the Department of Electronics and Communication Engineering, Dr. S. Mary Joans**, for her noble endeavor in encouraging our spirits to complete this project to the utmost satisfaction.

We are indebted to the undying support of our **Project Guide, Associate Professor, Dr. S. Manju** Department of Electronics and Communication Engineering, Velammal Engineering College for her continuous support and ideas through the course of the project.

Our special thanks to our **Project Coordinator, Dr. S. Manju, Associate Professor** for her constant guidance and suggestions to improve the project work.

Finally, we thank the teaching and non-teaching staff of our department, parents and friends who helped us in the successful completion of this project

## TABLE OF CONTENTS

<b>CHAPTER NO.</b>	<b>TITLE</b>	<b>PAGE NO.</b>
	<b>ABSTRACT</b>	<b>iv</b>
	<b>ACKNOWLEDGEMENT</b>	<b>v</b>
	<b>TABLE OF CONTENTS</b>	<b>vi</b>
	<b>LIST OF TABLES</b>	<b>viii</b>
	<b>LIST OF FIGURES</b>	<b>ix</b>
	<b>LIST OF ABBREVIATIONS</b>	<b>x</b>
<b>1</b>	<b>INTRODUCTION</b>	<b>1</b>
	1.1 ANTENNA IN WIRELESS COMMUNICATION	2
	1.2 TYPES OF ANTENNAS UTILIZED FOR WIRELESS COMMUNICATION	3
	1.3 BASIC THEORY OF MICROSTRIP ANTENNA	3
	1.4 BASIC OF MICROSTRIP ANTENNA	4
<b>2</b>	<b>LITERATURE SURVEY</b>	<b>6</b>
<b>3</b>	<b>PROPOSED WORK</b>	<b>9</b>
	3.1 SPIRAL PATCH ANTENNA OVERVIEW	9
	3.2 DESIGN EQUATIONS	10
	3.3 DESIGN AND DIMENSION EXPLANATION	12
	3.4 HFSS DESIGN AND FEED SETUP	17
	3.5 PERFORMANCE PARAMETERS	24
<b>4</b>	<b>HARDWARE AND SOFTWARE DETAILS</b>	<b>25</b>
	4.1 HARDWARE REQUIREMENTS	25
	4.1.1 Processor	25
	4.1.2 Memory (RAM)	25

4.1.3 Storage	25
4.1.4 Graphics Card	26
4.1.5 Display and Peripherals	26
4.1.6 Operating System	26
<b>4.1 SOFTWARE REQUIREMENTS</b>	<b>27</b>
4.2.1 Ansys hfss	27
4.2.2 Scripting and Automation Tools	28
4.2.3 Data Analysis and Visualization Tools	28
<b>5 EXPERIMENTAL RESULTS</b>	<b>29</b>
5.1 INTROUCTION	29
5.2 SIMULATION OVERVIEW	30
5.3 RETURN LOSS(S11) ANALYSIS	30
5.4 VSWR ANALYSIS	32
5.5 BANDWIDTH COMPARISON	34
5.6 GAIN AND DIRECTIVITY	35
5.7 RADIATION PATTERN	36
5.8 IMPEDANCE CHARACTERISTICS	37
5.9 PERFORMANCE COMPARISON SUMMARY	38
<b>6 CONCLUSION AND FUTURE SCOPE</b>	<b>40</b>
6.1 CONCLUSION	40
6.2 PHASE I WORK	41
6.3 PHASE II WORK	42
<b>REFERENCES</b>	

## LIST OF TABLES

<b>TABLE NO.</b>	<b>TITLE</b>	<b>PAGE NO.</b>
5.1	Antenna 1: Return Loss (S11) vs Frequency Values in dB	31
5.2	Antenna 2: Return Loss (S11) vs Frequency Values in dB	32
5.3	Antenna 2: VSWR vs Frequency Values in dB	33
5.4	Antenna 2: VSWR vs Frequency Values in dB	34
5.5	Values Of 3D Gain Plot	35
5.6	Values Of Directivity in Antenna 1 and Antenna 2	36
5.7	Radiation pattern output polarization in dB	37
5.8	summarizes the key performance parameters of both spiral antennas	38
5.9	Comparison between existing and proposed method	39

## LIST OF FIGURES

<b>FIGURE NO.</b>	<b>TITLE</b>	<b>PAGE NO.</b>
1.4	3D View of Microstrip patch antenna	5
3.1	Spiral patch antenna with 1.5mm Radius	10
3.2	ANSYS HFSS software 3D Model – Front View	22
3.3	ANSYS HFSS software 3D Model – Side View	23
3.4	ANSYS HFSS software 3D Model – Back View	23
3.5	ANSYS HFSS software 3D Model – Flat View	24
4.1	ANSYS HFSS software Logo	28
5.1	Spiral antenna with minimum width	30
5.2	Spiral antenna with maximum width	31
5.3	Antenna 1: Simulated Return Loss (S11) vs Frequency	31
5.4	Antenna 2: Simulated Return Loss (S11) vs Frequency	32
5.5	Antenna 1 -VSWR vs Frequency	33
5.6	Antenna 1 -VSWR vs Frequency	34
5.7	3D Gain Plot	35
5.8	Directivity of Antenna 1 and Antenna 2	36
5.9	Polar Plot – Radiation Pattern	38

## **LIST OF ABBREVIATIONS**

<b>HFSS</b>	High-Frequency Structure Simulator
<b>IEEE</b>	Institute of Electrical and Electronics Engineers
<b>WLAN</b>	Wireless Local Area Networks
<b>VoIP</b>	Voice over Internet Protocol
<b>WMAN</b>	Wireless Metropolitan Area Networks
<b>WLL</b>	Wireless Local Loop
<b>UWB</b>	Ultra-wide Band

# **CHAPTER 1**

## **INTRODUCTION**

Wireless communication is one of the fastest-growing and most innovative fields in today's communication industry. It involves the transfer of information between two or more points using electromagnetic waves, eliminating the need for physical wired connections. The roots of wireless communication can be traced back to the early twentieth century with the invention of radiotelegraphy, which used Morse code for the first wireless broadcasts. Since then, the field has evolved tremendously. During the 1950s and 1960s, major developments took place with the introduction of the cellular communication concept. The 1970s witnessed the invention of wired Ethernet and the foundation of modern networking. Further advancements such as second-generation (2G) digital cellular systems, satellite communication, and wireless internet technologies transformed global connectivity.

In the present era, wireless communication has become an integral part of everyday life and technological progress. It supports a wide range of applications, including Wireless Local Area Networks (WLAN), Zigbee for smart devices, Voice over Internet Protocol (VoIP) for internet-based calling, Wireless Metropolitan Area Networks (WMAN), and Wireless Local Loop (WLL) systems. Additionally, satellite communication enables global broadcasting, GPS navigation, and remote communication. The continuous evolution of wireless technology has made communication faster, more efficient, and more accessible across the world.

## **1.1 ANTENNA FOR WIRELESS COMMUNICATION**

Antenna is one of the key components in wireless communication systems. An antenna is an IEEE standard aerial designed to radiate or receive radio waves. All antennas are working based on electromagnetic theory. Computer architecture and technology play dominant role in advancing modern antenna technology. In the mid-19th century, there is a significant shift in antenna technology improvement. The antenna impedance bandwidth enhancement technology is as high as 40:1 or more. The geometries of these wideband antennas are being specified by angles, rather than by linear dimensions.

The main applications of these wideband antennas are high-gain radar communication, point-to-point communication. It introduced a new radiating element. Many applications with great ease of manufacture were found compared with the older design patch antenna. These antennas help the active elements to communicate with one another. A range of antenna characteristics namely gain, radiation pattern, and dimension of main element can be controlled electronically. In recent years, significant progress has been made in the production of millimeter wave antennas.

Active and passive circuitry with radiating elements are combined in one compact unit. Intelligent antennas that are called adaptive arrays introduced in the same way. It includes algorithms for signal processing. These antennas allow for easy integration with state-of-the-art digital systems. Antennas are the key components of every communication system. They connect a transmitter to a free space, then free space to a receiver. The antennas act like a transducer between a guided wave and free space. Antenna is a step in the way of successful communication among any device

## **1.2 TYPES OF ANTENNAS UTILIZED FOR WIRELESS COMMUNICATION**

Antennas are widely divided into:

- Wire Antenna
- Aperture Antenna
- Corner Antenna
- Dipole Antenna
- Printed Antenna

In cars, buildings, radio receiver units, warships and aircraft antennas are frequently used. It includes classical antenna types like dipole, loop, helix, etc. Loop antennas are a category for wire antennas. It can be done as square, triangle, rectangle and circular loops in different forms. In loop antenna, circular loop antenna is the most common. It has a simple construction. Aperture antennas are the best candidates for applications in aircraft and space where antennas must be installed on the surface of big craft.

Antenna arrays are used by replacing a single antenna element for improving the radiation characteristics in the desired direction. Planar antennas are compatible with the design of a Monolithic Integrated Microwave Circuit (MMIC). Printed antennas with modern printed circuit technology are easier and cost efficient to manufacture. They are low profile and compatible with flat and non-flat surfaces. Microstrip Patch Antenna is one of the most popular printed antennas.

## **1.3 ANTENNA DESIGN CHALLENGES**

An antenna design engineer lacks design challenges depending on the application addressed, mechanical and electric characteristics and operating system cost. The design of antenna for any wireless network requires a variety of technical challenges.

First of all, there is a limited electromagnetic spectrum needed for various wireless communication appliances. The lower frequency range is overcrowded already and requires the systems and devices that can perform well with the same cost and performed in the microwave range. Secondly, the low-volume, low-profile and lightweight compactness of the antenna is preferable for the small space of Bluetooth, Global Satellite Positioning System (GPS), Wireless Fidelity (Wi-Fi) and worldwide interoperability for microwave access (WiMAX) devices. Therefore, in integrated systems it is highly necessary to design a compact antenna. The implementation of more than one communication application on a single compact device is another significant challenge in antenna design. This requires compact and multiband antennas to be designed. The maintenance of a high isolation between the adjacent operating bands is an important constraint in multi-band antenna design in order to reduce the interference between them.

Additional challenges in the design of multi-band antennas are the development of commercial and military applications. The freedom of alignment between the receiver and the transmitter is required. One of the most important challenges, is the design of a multi-band antenna with multi polarized characteristics. In addition to multi-band operation, antenna design is concerned by the gain, efficiency and radiation patterns.

#### **1.4 BASIC OF MICROSTRIP ANTENNA**

The Microstrip antenna is one of the most popular types of printed antenna. They have a very significant role to play in today's wireless communication systems. The microstrip antenna is divided into four: microstrip patch antennas, microstrip dipoles, a printed slot antenna and a microstrip travelling-wave antenna. In this thesis, the microstrip patch antennas and microstrip dipoles are used. The patch antenna is geometrically radiated; square, triangular, rectangular, circular, elliptical, sectoral, annular etc. The commonly used type for design, fabricate and easy analysis is

rectangular microstrip antenna. Many advantages have been overcome in the conventional microwave antennas by the use of the microstrip antenna. The big drawback of the microstrip antenna is a narrow impedance bandwidth of 1-2%, it has low gain, lower frequencies importability and sometimes undesirable radiation patterns.

Figure 1.4 shows the simple microstrip patch antenna. This antenna consists of a radiating element on one side and a dielectric substrate on the other side, known as the ground plane. The signal is coupled to the main radiating element by any one of the feeding techniques. Microstrip antennas are widely used in modern wireless systems. It is compact compared to conventional microwave antennas.

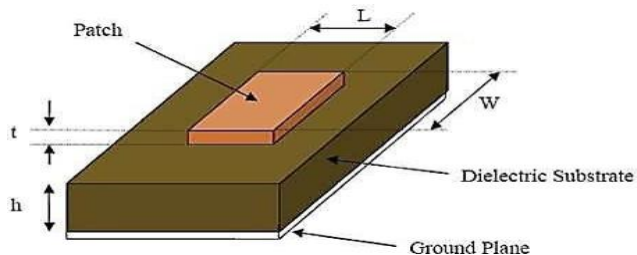


Figure 1.4 3D View of Microstrip patch antenna

### **Microstrip antennas' general characteristics are**

- Low volume and lightweight
- Low profile planar configuration, so wireless boards can be easily mounted
- Manufacturing costs is low, which makes manufacturing easy
- Easily integrated with integrated microwave circuits
- Operates for dual and triple bands with two orientations
- Linear and circular polarizations with feed techniques are present.

## CHAPTER 2

### LITERATURE SURVEY

- 1. Sherburne, M., Sibert, K., Daffron, M., Lennon, A., Feldmesser, H., Furer, J., Wolff, K., Pionke, K., Biermann, P., Bettwy, L., Eby, D., Hebert, C., Gonzalez, S., Grim, D., Storck, S., & Hollenbeck, J. (2025). “Two-Way Additively Manufactured Shape Memory Alloy Wideband Reconfigurable Compound Antenna.” *ACS Applied Engineering Materials*, 3(1), 44–50.**

A paradigm shifting antenna technology taking advantage of recent advancements in additive manufacturing is presented for the first time. Fine control over additive manufacturing has allowed fabrication of a two-way shape memory alloy antenna. A double spiral antenna capable of actuating through thermal response alone is able to actuate from a flat spiral antenna to an extended conical spiral antenna. Actuation control was achieved by measuring changes in electrical resistance caused by shape Memory alloy phase changes. The prototype antenna was validated from 4GHz to 11GHz (S to X Bands) with a gain of S to X bands) with a gain of approximately 5dBi. The measured trends in antenna gain as a function of frequency from the actuation agree with simulations.

- 2. Liu, H., Zhang, Y., & Zhao, X. (2023). “A Ku Wideband Circularly Polarized Microstrip Antenna Array with Low Profile Crossed-Dipole Element.” *International Journal of Antennas and Propagation*, 2023.**

This work introduces a novel Ku-band wideband CP antenna array using crossed-dipole elements (CDE) with sequential rotation (SR) feeding. A unique low-profile, heart-shaped patch dipole design combined with a metal via feeding structure eliminates soldering issues at high frequencies. The fabricated 2×2 array achieved an

impedance bandwidth of 44% (11.6–18.15 GHz), an axial ratio bandwidth of 38.7% (12–17.65 GHz), and a peak gain of 11.02 dBi at 14 GHz, making it well-suited for satellite communication and high-frequency applications.

3. Krishna Jyothi, N., Kumudini, M., Sowmya, B., Akhila Yadav, N., & Sai Nikitha, P. (2023). "Design and Simulation of Elliptical Shaped Microstrip Patch Antenna Using HFSS." *International Journal for Research in Applied Science & Engineering Technology (IJRASET)*, 11(11), 259–266.

This research presents a comprehensive study on the design, fabrication, and performance analysis of an elliptical patch antenna operating at 2.4 GHz using FR4 substrate material. The elliptical shape was chosen for its unique radiation characteristics and compact form factor, making it suitable for integration into modern wireless communication systems including Wi-Fi, Bluetooth, and IoT devices. Advanced simulation using ANSYS HFSS electromagnetic simulator was employed to optimize the antenna's performance, achieving desirable characteristics such as low return loss and enhanced bandwidth. The proposed antenna demonstrates promising applications in the 2.4 GHz frequency band with robust performance for space-constrained wireless communication applications. The key findings include optimized antenna parameters with return loss ( $S_{11}$ ) characteristics, VSWR performance, and radiation pattern analysis that validate the antenna's suitability for wireless communication systems operating in the ISM band.

**4. Li, W., Xue, W., Li, Y., Chung, K. L., & Huang, Z. (2023). "A Wideband Differentially Fed Circularly Polarized Slotted Patch Antenna with a Large Beamwidth." *Journal of Electromagnetic Engineering and Science*, 23(6), 512–520.**

This research presents a novel differentially fed circularly polarized (CP) antenna featuring a slotted patch design with exceptional beamwidth characteristics. The antenna design involves coupling a differential bending dipole antenna to a slotted patch in the same plane to achieve high gain and wide axial ratio (AR) bandwidth. The structure utilizes F4BM material ( $\epsilon_r = 2.2$ ) for Layer 1 and Rogers 4003C ( $\epsilon_r = 3.55$ ) for Layer 2, with Computer Simulation Technology (CST) Microwave software for optimization. The measured results demonstrate impressive broadband performance with a -10-dB impedance bandwidth of 78.8% (3.81–8.76 GHz), a 3-dB AR bandwidth of 36.7% (4.78–6.93 GHz), and a maximum gain of 10.2 dBic. The antenna achieves remarkable AR beamwidths of  $132.3^\circ$  in the xoz plane and  $116.2^\circ$  in the yoz plane at 5.5 GHz, significantly outperforming traditional CP antennas in terms of coverage area and bandwidth characteristics

## CHAPTER 3

### PROPOSED WORK

In this chapter, the design and implementation of an Archimedean Spiral Patch Antenna operating in the 12–18 GHz frequency band are presented. The antenna is designed using an FR4 substrate of dimensions  $40\text{ mm} \times 50\text{ mm} \times 1.6\text{ mm}$ . The Archimedean spiral structure is chosen for its ability to provide broadband characteristics and circular polarization. Such antennas find applications in modern communication systems, including radar, satellite communication, and ultrawideband (UWB) systems.

#### **3.1 SPIRAL PATCH ANTENNA OVERVIEW**

Spiral antennas are a class of frequency-independent antennas known for their broad bandwidth and stable radiation patterns across a wide range of frequencies. Among them, the Archimedean spiral antenna is one of the most popular designs due to its simple geometry, easy fabrication, and predictable input impedance. It consists of two or more conducting arms wound around a common central point, with a constant spacing between each turn. This uniform spacing helps maintain consistent performance over a wide frequency range. The antenna typically operates in the self-complementary mode, which ensures wideband impedance matching, often close to  $188.5\Omega$ . One of its key advantages is that it produces circularly polarized radiation, making it ideal for communication systems that require polarization diversity. Circular polarization minimizes multipath interference and signal fading, improving the reliability of wireless links. Hence, the Archimedean spiral antenna is widely used in radar, satellite, and broadband communication applications.

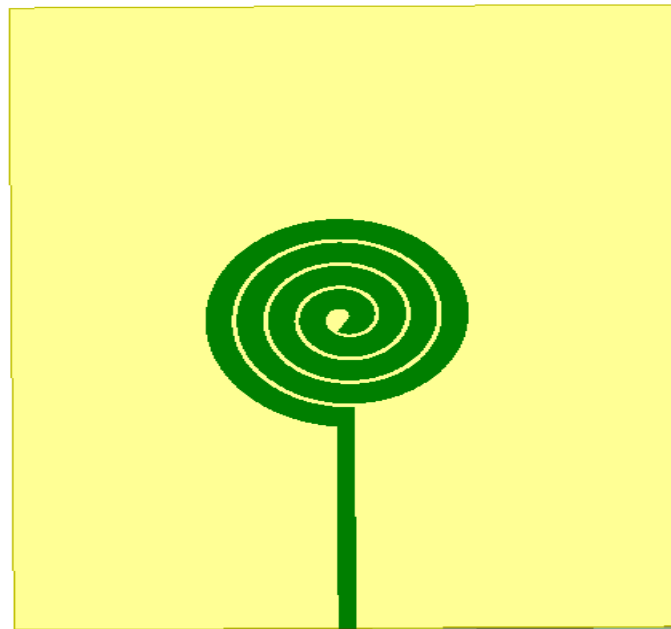


Figure 3.1 Spiral patch antenna with 1.5mm Radius

The spiral antenna can operate over a wide frequency band determined by its inner and outer radii. At lower frequencies, the outer radius defines the minimum frequency of operation, while the inner radius defines the upper limit. For printed or planar implementations, the antenna is fabricated on a dielectric substrate such as FR4, which influences the resonant behavior and bandwidth.

### 3.2 DESIGN EQUATIONS

The Archimedean spiral is described by the polar coordinate equation:

$$\mathbf{r} = \mathbf{r}_0 + a\theta$$

where:

$r$  – radial distance from the center (mm)

$r_0$  – starting radius (mm)

$a$  – growth rate of the spiral (mm/rad)

$\theta$  – angular position (radians)

The total length of the spiral arm can be estimated using:

$$L = \int \sqrt{r^2 + (dr/d\theta)^2} d\theta$$

For an Archimedean spiral, this simplifies to:

$$L = a/2 [\theta\sqrt{1 + \theta^2} + \sinh^{-1}(\theta)]$$

The operating frequency band of the spiral antenna is approximated by:

$$f_{\text{low}} \approx c / (2\pi R_{\text{out}} \sqrt{\epsilon_{\text{eff}}})$$

$$f_{\text{high}} \approx c / (2\pi R_{\text{in}} \sqrt{\epsilon_{\text{eff}}})$$

where:

- $R_{\text{out}}$  – outer radius of the spiral (mm)
- $R_{\text{in}}$  – inner radius (mm)
- $\epsilon_{\text{eff}}$  – effective permittivity of the substrate
- $c$  – speed of light in free space ( $3 \times 10^8$  m/s)

The Archimedean spiral antenna works on the principle of a gradually expanding spiral shape, where the distance between turns remains constant. This geometry allows the antenna to operate over a wide range of frequencies, making it a broadband radiator. The spiral structure supports circular polarization, providing consistent performance regardless of signal orientation. The spiral arms guide the current smoothly, resulting in stable radiation patterns. Because of these features, it is widely used in radar, satellite, and wideband communication systems.

### **3.3 DESIGN AND DIMENSION EXPLANATION**

The antenna is designed on an FR4 substrate with dielectric constant  $\epsilon_r = 4.4$  and thickness  $h = 1.6$  mm. The substrate size is chosen as  $40\text{ mm} \times 50\text{ mm}$  to accommodate the spiral geometry and ensure minimal edge reflections. The spiral arm width is set to 1.5 mm to balance between radiation efficiency and impedance matching.

The following parameters are considered during design:

- Substrate: FR4 ( $\epsilon_r = 4.4$ ,  $\tan\delta = 0.02$ )
- Substrate dimensions:  $40\text{ mm} \times 50\text{ mm} \times 1.6\text{ mm}$
- Spiral arm width (w): 1.5 mm
- Inner radius ( $r_0$ ): 3 mm
- Outer radius (R): 20 mm
- Number of turns: 2.5
- Feed type: Coaxial probe feed at spiral center

#### **Substrate Selection and Properties:**

The choice of substrate plays a major role in defining the performance of microstrip and spiral antennas. In this design, FR4 epoxy is selected as the substrate material because it offers a good balance between cost, mechanical strength, and dielectric performance. FR4 has a dielectric constant ( $\epsilon_r$ ) of 4.4 and a loss tangent ( $\tan\delta$ ) of 0.02, which indicates moderate dielectric losses suitable for low-cost RF applications. The substrate thickness ( $h = 1.6$  mm) is chosen as a standard PCB thickness that provides structural stability while preventing excessive surface waves.

The dielectric constant determines the wavelength reduction factor inside the substrate, given by:

$$\lambda_{eff} = \frac{\lambda_0}{\sqrt{\epsilon_{eff}}}$$

where  $\epsilon_{eff}$  is the effective dielectric constant. A higher  $\epsilon_r$  results in a smaller wavelength, allowing the antenna to be compact. However, too high a dielectric value can confine energy within the substrate, reducing radiation efficiency. Hence, FR4's moderate  $\epsilon_r = 4.4$  gives a practical compromise between miniaturization and performance.

### Spiral Geometry and Equation:

The heart of this design is the spiral radiator, which determines the operating frequency and radiation pattern. A planar Archimedean spiral is used, defined by the equation:

$$r = r_0 + a\theta$$

where:

- $r_0$  = starting (inner) radius
- $a$  = growth rate of the spiral
- $\theta$  = angular displacement (in radians)

For this antenna, the inner radius ( $r_0$ ) = 3 mm and the outer radius ( $R$ ) = 20 mm, allowing 2.5 turns of the spiral arm within the 50 mm substrate length.

The number of turns ( $N$ ) defines the antenna's bandwidth and impedance behaviour. More turns typically increase the effective length, improving gain and low-frequency operation, but also increase the overall size. Here,  $N = 2.5$  turns ensures a compact yet broadband operation.

The spiral arm grows gradually outward, maintaining a constant spacing between turns, which supports circular polarization and wideband performance.

### **Spiral Arm Width:**

The width of the spiral arm ( $w = 1.5$  mm) is another critical parameter. The arm width controls the current distribution and impedance matching. If the width is too narrow, conductor losses increase, leading to reduced efficiency. Conversely, if it is too wide, the antenna may detune and alter its radiation characteristics. The chosen 1.5 mm width offers a good balance between surface current flow and structural rigidity.

The arm width also influences the spacing between turns. Proper spacing minimizes coupling between adjacent arms, ensuring stable radiation and maintaining the intended frequency response.

### **Feed Configuration:**

The feed configuration plays a crucial role in determining the performance of a spiral antenna. In this design, the antenna is excited using a coaxial probe feed located at the center of the spiral. This feeding mechanism ensures that both spiral arms are excited symmetrically, resulting in balanced current distribution and enhanced radiation efficiency.

A coaxial feed consists of an inner conductor, dielectric insulator, and an outer conductor (shield). The inner conductor carries the RF signal to the antenna, while the outer conductor connects to the ground plane, providing proper shielding to prevent unwanted radiation.

In the proposed spiral antenna:

- The inner conductor connects to the central point of the spiral.
- The outer conductor is soldered to the ground plane at the bottom of the substrate.
- The feed passes vertically through the FR4 substrate (thickness = 1.6 mm).

This configuration helps achieve a  $50 \Omega$  impedance match between the feed and the antenna structure, allowing efficient power transfer with minimal reflection.

The characteristic impedance ( $Z_0$ ) of a coaxial cable is given by:

$$Z_0 = \frac{60}{\sqrt{\epsilon_r}} \ln \left( \frac{D}{d} \right)$$

where,

$\epsilon_r$ = Dielectric constant of the substrate (FR4 = 4.4)

$D$ = Inner diameter of the outer conductor (mm)

$d$ = Diameter of the inner conductor (mm)

To maintain a  $50 \Omega$  impedance, the ratio  $\frac{D}{d}$  must satisfy:

$$\frac{D}{d} = e^{\frac{Z_0 \sqrt{\epsilon_r}}{60}}$$

This equation is used during the feed design to calculate the proper diameters of the inner and outer conductors for impedance matching. Maintaining  $Z_0 = 50 \Omega$  minimizes the reflection coefficient ( $\Gamma$ ) and improves power transmission.

The reflection coefficient is expressed as:

$$\Gamma = \frac{Z_{in} - Z_0}{Z_{in} + Z_0}$$

and the return loss ( $S_{11}$ ) is given by:

$$S_{11} = -20\log_{10} |\Gamma|$$

A well-matched feed ensures  $S_{11} < -10$  dB, which indicates that more than 90% of the input power is effectively radiated by the antenna. The feed is placed exactly at the center of the spiral geometry, allowing equal excitation of both arms. This symmetry ensures:

- Circular polarization of the radiated wave.
- Uniform radiation pattern.
- Wide impedance bandwidth due to reduced phase imbalance.

If the feed were offset from the center, one arm would receive more current, leading to distorted radiation and degraded polarization quality. The coaxial probe passes through the FR4 substrate and is modeled in HFSS as a metallic cylinder with perfect electric conductivity (PEC).

- The inner conductor touches the spiral's inner end.
- The outer conductor connects to the ground plane.

This maintains proper electrical continuity between the feed and antenna body.

In ANSYS HFSS, parameters like probe diameter, feed position, and substrate thickness are optimized using the Optimetrics tool to achieve:

- Minimum  $S_{11}(< -10 \text{ dB})$
- Proper impedance matching ( $\approx 50 \Omega$ )
- Symmetrical current distribution

### 3.4 HFSS DESIGN AND FEED SETUP

Designing and analyzing the proposed spiral antenna in ANSYS HFSS (High-Frequency Structure Simulator) involves a series of structured steps that define the substrate, radiator geometry, feeding mechanism, and boundary conditions. Each of these steps plays a crucial role in ensuring the antenna operates at the desired frequency with efficient radiation characteristics. The overall design procedure is summarized below.

#### Creation of the Substrate:

The first step in the HFSS model involves creating the dielectric substrate that forms the base of the antenna structure. The substrate serves as a mechanical support for the radiating spiral and influences the antenna's electrical characteristics such as impedance, bandwidth, and gain. A rectangular substrate of size  $40 \text{ mm} \times 50 \text{ mm} \times 1.6 \text{ mm}$  is created using the "Box" or "Rectangle" tool in HFSS's 3D Modeler environment. These dimensions are chosen based on the desired operating frequency and the space required for the spiral arms. The thickness of 1.6 mm corresponds to standard FR4 substrate material, which is widely used due to its cost-effectiveness and moderate dielectric properties (dielectric constant  $\epsilon_r \approx 4.4$ ). In the Modeler window, the origin  $(0,0,0)$  is often used as a reference point for the substrate's center to simplify later

geometric alignment steps. The coordinate system ensures that the top face lies along the XY-plane, where the spiral radiator will be placed.

### **Defining the Spiral Structure:**

Once the substrate is created, the next step is to design the spiral radiator. The spiral structure is defined mathematically using the equation  $r = r_0 + a\theta$ , where  $r_0$  is the starting radius,  $a$  is the growth rate (defining the spacing between turns), and  $\theta$  represents the angular rotation in radians. Using this equation, a parametric curve can be generated in HFSS by specifying points along the spiral path. The curve is then swept with a rectangular profile to form a 3D copper strip representing the radiating arm. The width of the spiral arm is maintained at 1.5 mm, ensuring proper current distribution and impedance characteristics. Two identical spiral arms are created and placed 180° apart, maintaining symmetry in the structure. This dual-arm configuration improves radiation efficiency and provides circular polarization when excited properly. Special care is taken to maintain continuous connectivity of the spiral's inner and outer ends for proper feed placement.

### **Ground Plane Formation:**

A ground plane is essential for establishing a reference potential and reflecting electromagnetic waves to reinforce radiation in the desired direction. In HFSS, a copper sheet is defined on the bottom face of the substrate, covering the entire 40 mm × 50 mm area. This ground plane serves two main functions: it provides a return path for the current from the feed probe and controls the radiation pattern of the antenna. By acting as a reflector, the ground ensures that most of the radiation is directed away from the substrate, resulting in improved gain and reduced back lobes. The thickness of the copper ground is typically set to 0.035 mm, which is the standard

copper cladding thickness in PCB fabrication. The ground material is later assigned the Copper ( $\sigma = 5.8 \times 10^7$  S/m) property from HFSS's material library.

### **Coaxial Probe Feed Design:**

Feeding is a crucial part of antenna design, as it determines how efficiently power is transferred from the transmission line to the radiating structure. In this design, a coaxial probe feed is used because of its simplicity and ease of integration in printed antennas. A coaxial structure consists of an inner conductor, dielectric layer, and outer conductor (shield). In HFSS, this feed is modeled by inserting a coaxial cylinder through the substrate's center. The inner conductor of the coaxial feed is connected to the inner end of the spiral, while the outer conductor is connected to the ground plane. The feed dimensions are chosen to achieve a characteristic impedance of  $50 \Omega$ , which matches the impedance of standard RF measurement equipment. Typically, the coaxial dielectric (Teflon or air) has a dielectric constant close to 2.1, and the inner and outer diameters are adjusted accordingly. Proper feed alignment and meshing refinement at the probe junction are important to minimize simulation errors and ensure accurate S-parameter results.

### **Defining Radiation Boundaries:**

To simulate realistic antenna behavior, it is essential to define radiation boundaries that emulate free-space conditions. In HFSS, this is done by enclosing the entire antenna structure within an airbox. The airbox acts as a volume in which electromagnetic waves can propagate freely, preventing unwanted reflections from the simulation boundaries. The airbox is typically extended by a clearance of  $\lambda/4$  (quarter wavelength) from the antenna in all directions, where  $\lambda$  corresponds to the wavelength at the operating frequency. For example, if the antenna operates around 2.4 GHz,  $\lambda \approx 125$  mm, and hence the airbox should extend at least 31 mm beyond the antenna edges.

After creating the airbox, its surface is assigned as a “Radiation Boundary” in HFSS. This boundary type ensures that outgoing waves are absorbed, mimicking an infinite free-space environment.

In some cases, a Perfectly Matched Layer (PML) boundary can be used for more accurate results, especially for broadband simulations. Correctly defining these boundaries prevents reflection errors and ensures reliable calculation of far-field radiation patterns and antenna parameters such as gain, directivity, and efficiency.

### **Material Assignment:**

Material properties greatly influence antenna performance, especially in determining resonance frequency and impedance. In HFSS, appropriate materials are assigned to each part of the design:

- Substrate: Assigned as FR4\_epoxy with dielectric constant ( $\epsilon_r$ ) of 4.4 and loss tangent of 0.02.
- Spiral and Ground Plane: Assigned as Copper, with electrical conductivity  $\sigma = 5.8 \times 10^7$  S/m.
- Coaxial Dielectric: Assigned as Teflon (PTFE) with  $\epsilon_r = 2.1$ , if modeled explicitly.
- Airbox: Assigned as Air, representing free-space conditions.

These material settings are applied using HFSS’s “Assign Material” tool. Correct assignment ensures the simulation reflects real-world physical conditions. Losses due to dielectric and conductor properties are automatically included during S-parameter and radiation analysis.

## **Meshing and Simulation Setup:**

After defining the geometry and boundaries, HFSS automatically generates a finite element mesh that divides the model into small tetrahedral elements. Finer meshing is applied near critical regions such as the feed point, spiral edges, and substrate interfaces to ensure numerical accuracy. An adaptive meshing process is performed, where the mesh is refined iteratively until convergence is achieved. Once meshing is complete, a solution setup is defined specifying the operating frequency range (for example, 2 GHz to 6 GHz). Finally, S-parameters and far-field radiation patterns are computed. The reflection coefficient ( $S_{11}$ ) helps identify the resonant frequency and impedance matching quality, while the radiation pattern provides insights into antenna directionality and polarization.

## **Summary of the HFSS Design Workflow:**

The HFSS design and feed setup process plays a crucial role in accurately modeling every essential aspect of the antenna, including its geometry, feeding mechanism, material properties, and boundary conditions within the simulation environment. Each of these elements is carefully defined to ensure that the antenna operates efficiently and delivers precise, reliable performance results. By combining the mathematical design equation ( $r = r_0 + a\theta$ ) with practical simulation tools in HFSS, designers can effectively analyze and optimize the antenna's behavior across different frequency ranges. This powerful integration enables the prediction of real-world performance without the need for immediate physical testing. Consequently, it minimizes the number of fabrication trials, thereby significantly reducing prototyping costs and development time. Moreover, this systematic and analytical approach enhances the overall accuracy, efficiency, and reliability of the final antenna design, ensuring that it performs as expected when implemented in practical applications.

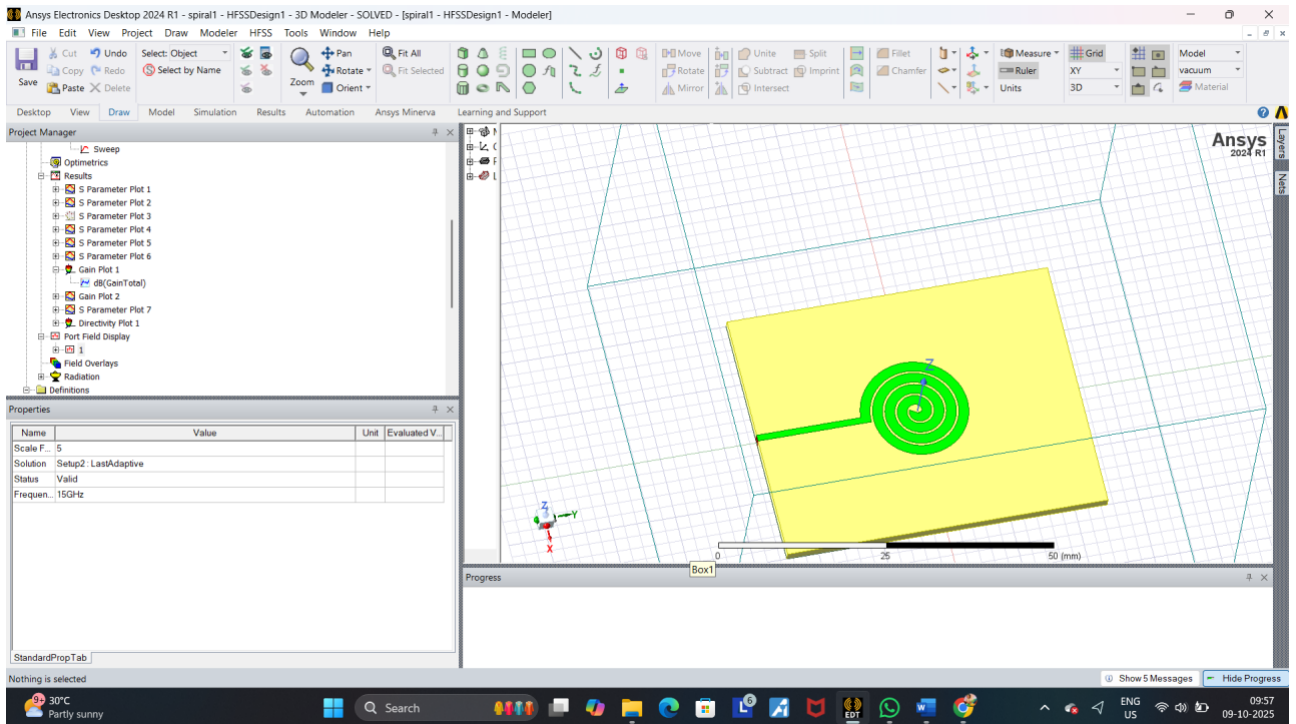


Figure 3.2: ANSYS HFSS software 3D Model – Front View

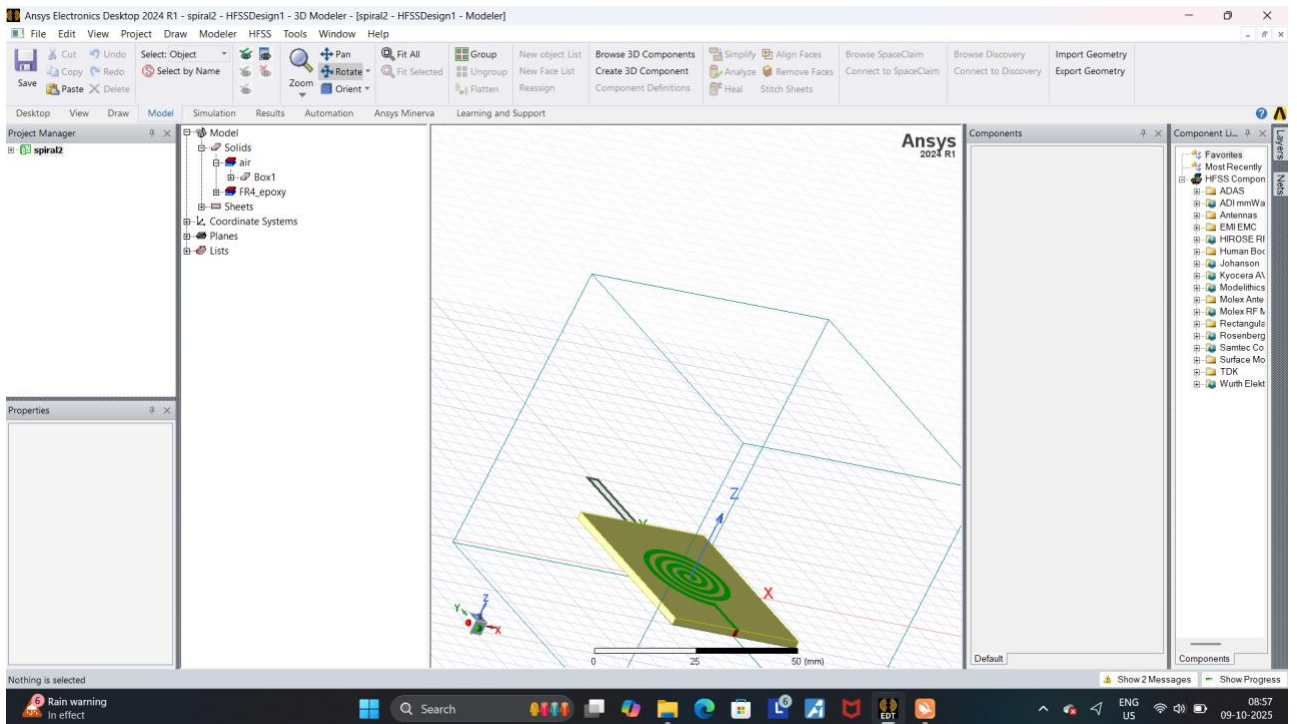


Figure 3.3: ANSYS HFSS software 3D Model – Side View

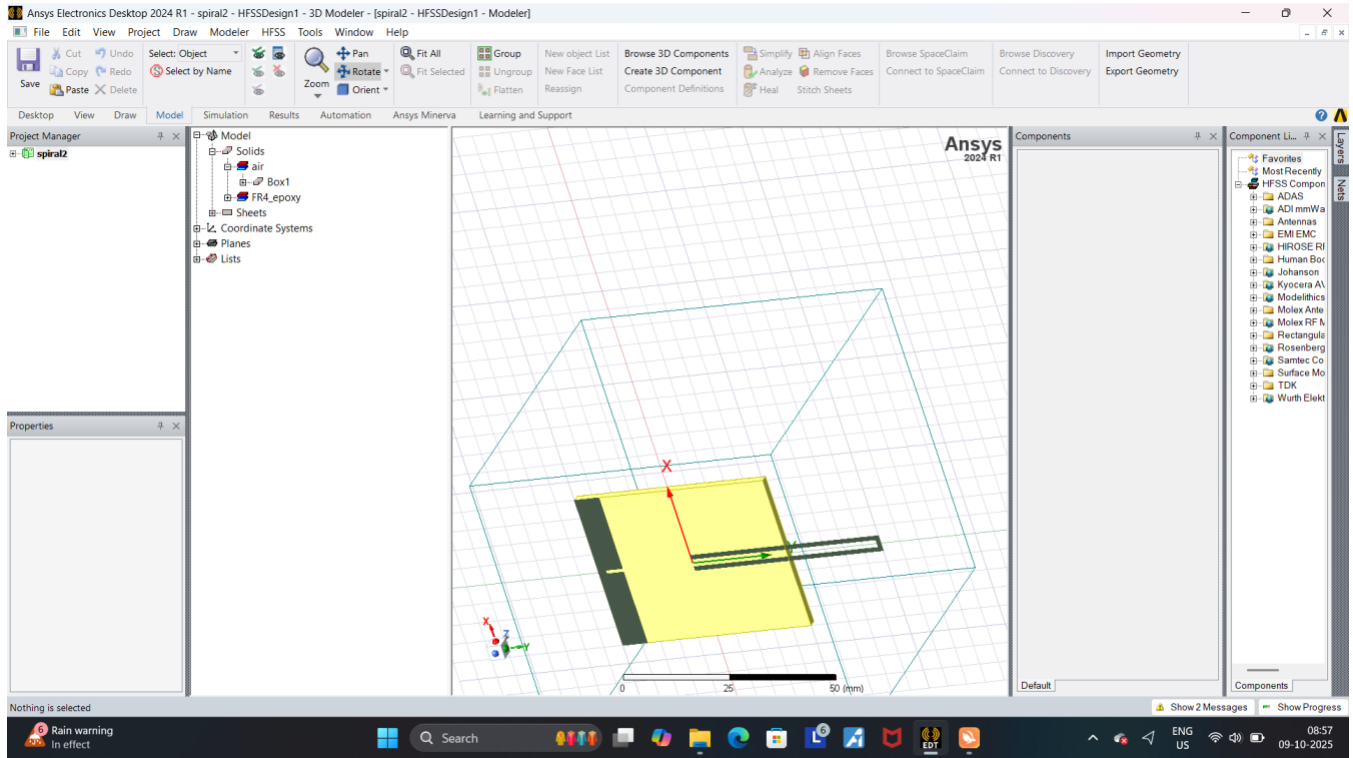


Figure 3.4: ANSYS HFSS software 3D Model – Back View

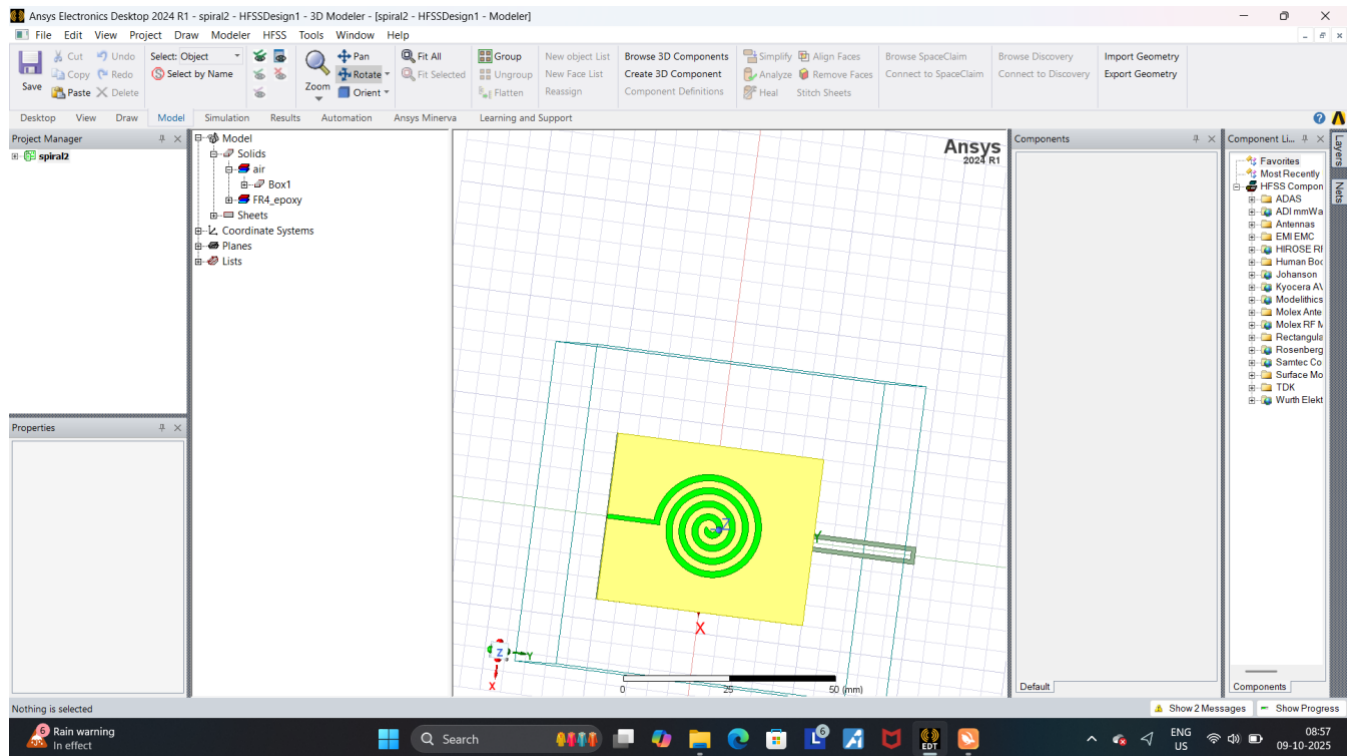


Figure 3.5: ANSYS HFSS software 3D Model – Flat View

### **3.5 PERFORMANCE PARAMETERS**

The designed spiral patch antenna is expected to exhibit broadband behavior with return loss better than -10 dB across 12–18 GHz. Circular polarization can be achieved due to the dual-arm spiral configuration. Typical simulated parameters include:

- Bandwidth: 6 GHz (12–18 GHz)
- Return Loss ( $S_{11}$ ): < -10 Db
- Gain: 4–6 dBi
- Axial Ratio: < 3 dB
- Radiation pattern: Bidirectional or unidirectional depending on backing round plane design

The design of an Archimedean spiral patch antenna operating in the 12–18 GHz band has been successfully carried out. Using FR4 substrate and a spiral geometry, the antenna achieves broadband characteristics with stable radiation patterns. The inclusion of HFSS simulation setup ensures practical implementation feasibility. This antenna structure is highly suitable for modern broadband communication systems requiring compactness and wide operational bandwidth.

# **CHAPTER 4**

## **HARDWARE AND SOFTWARE DETAILS**

### **4.1 HARDWARE REQUIREMENTS**

#### **4.1.1 Processor**

The processor is the central unit that performs all computational tasks during antenna simulation. A high-performance processor such as an Intel Core i7/i9 or AMD Ryzen 7/9 ensures faster meshing and frequency sweep calculations in ANSYS HFSS. Multi-core processors improve efficiency when handling complex 3D electromagnetic problems.

#### **4.1.2 Memory (RAM)**

Random Access Memory (RAM) is essential for storing temporary data during simulation runs. At least 16 GB of RAM is required, but 32 GB is recommended for adaptive mesh refinement and broadband frequency analyses. Sufficient memory ensures smoother operation and prevents simulation crashes during large model computations.

#### **4.1.3 Storage**

Fast storage significantly affects simulation performance, especially when saving or reading large project files. A Solid-State Drive (SSD) with a minimum capacity of 512 GB provides quick data access and reduces simulation loading times. Using SSDs also enhances reliability and system responsiveness during result processing.

#### **4.1.4 Graphics Card**

A powerful graphics card with OpenGL support is necessary to visualize 3D antenna models and field distributions effectively. GPUs such as NVIDIA GTX 1660 or RTX 3060 enable smooth rendering of the simulation environment. This ensures clear visualization of current distributions, radiation patterns, and structure geometry.

#### **4.1.5 Display and Peripherals**

A full HD display ( $1920 \times 1080$ ) or higher resolution is recommended for detailed model inspection. Standard peripherals like a keyboard and mouse are required for navigation and model control. Optionally, a 3D mouse can be used to manipulate complex structures with higher precision and ease.

#### **4.1.6 Operating System**

ANSYS HFSS requires a stable 64-bit operating system for optimal performance. Windows 10 or Windows 11 (64-bit) are recommended due to their compatibility and support for simulation tools. The operating system ensures efficient resource management and smooth execution of high-performance tasks.

## **4.2 SOFTWARE REQUIREMENTS**

### **4.2.1 ANSYS HFSS**

ANSYS HFSS (High Frequency Structure Simulator) is a powerful electromagnetic simulation software widely used for designing and analyzing antennas, RF components, and microwave devices. It provides precise 3D modeling and full-wave electromagnetic field analysis using the finite element method (FEM). In antenna design, HFSS helps engineers visualize and optimize critical parameters such as radiation patterns, field distributions, return loss ( $S_{11}$ ), VSWR, and gain before physical fabrication. The software allows users to perform frequency sweeps, parametric studies, and optimization to achieve the desired performance over a broad frequency range. For the spiral antenna, HFSS accurately models the geometry, material properties, and feed structure, ensuring reliable results that closely represent real-world behavior.

It also supports boundary conditions and adaptive meshing to enhance simulation accuracy. Overall, HFSS plays a vital role in predicting antenna efficiency, minimizing design errors, and reducing prototyping costs by validating performance virtually before implementation.



Figure 4.1 ANSYS HFSS software Logo

#### **4.2.2 Scripting and Automation Tools**

These tools enable parametric modeling, optimization, and batch processing of multiple antenna variations. Automation reduces human error and significantly enhances design productivity.

#### **4.2.3 Data Analysis and Visualization Tools**

After obtaining the simulation output from HFSS or other electromagnetic solvers, these software tools are used to plot key performance parameters such as S11 (return loss), VSWR (Voltage Standing Wave Ratio), gain, and radiation patterns. These graphical representations provide a clear understanding of how efficiently the antenna operates across different frequencies.

MATLAB enables advanced data manipulation and automation of result analysis through scripting, while Excel offers easy tabulation, filtering, and charting of data for quick interpretation. By observing these plots, designers can identify performance trends, mismatches, or losses and make necessary design adjustments. This post-processing analysis is essential for optimizing antenna parameters, ensuring the design meets desired specifications. Thus, integrating MATLAB or Excel in the design workflow enhances accuracy, efficiency, and decision-making during antenna development.

# CHAPTER 5

## EXPERIMENTAL RESULTS

### 5.1 INTRODUCTION

This chapter presents the simulation results and performance comparison of two designed Archimedean spiral patch antennas. Both antennas are designed using the same substrate material (FR4) and dimensions but differ in the spacing between spiral arms. Antenna 1 features a smaller inter-arm gap, while Antenna 2 incorporates a larger spacing between arms. The effect of spiral arm spacing on key antenna performance parameters such as return loss, bandwidth, gain, directivity, and VSWR is analyzed using ANSYS HFSS simulation results.

Antenna performance in figure 4.a and 4.b are investigated and results are discussed in this chapter. The coat used is of a dielectric material (FR4: 4.4). Both of the antennas are tuned to work at around ku band.

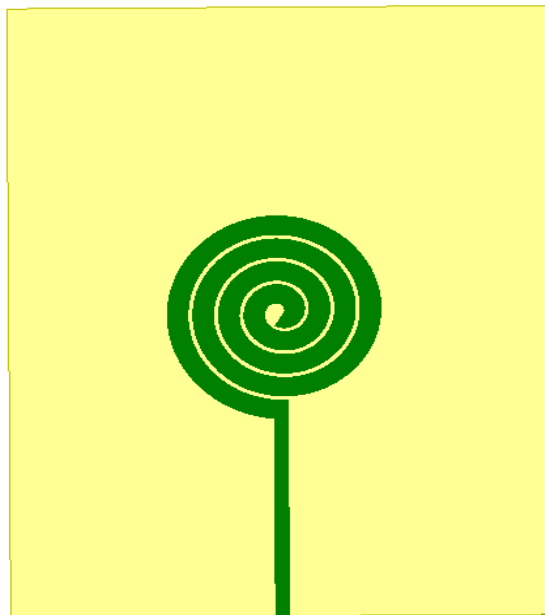


Figure 5.2: Spiral antenna with minimum width

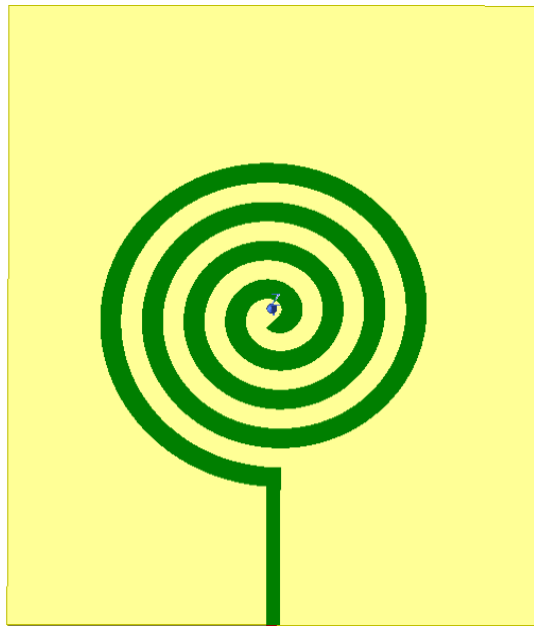


Figure 5.1: Spiral antenna with maximum width

## 5.2 SIMULATION OVERVIEW

The antennas were simulated in ANSYS HFSS 2022 R1 using a finite element method (FEM) solver. The simulation setup included a coaxial feed, FR4 substrate ( $\epsilon_r = 4.4$ , thickness = 1.6 mm), and airbox with  $\lambda/4$  boundary. Frequency sweep was performed from 12 GHz to 18 GHz with adaptive meshing for improved accuracy. The simulated S11, VSWR, gain, and radiation characteristics were extracted and compared between the two antenna structures.

## 5.3 RETURN LOSS (S11) ANALYSIS

Return loss represents the amount of power reflected due to impedance mismatch at the feed point. A lower return loss value indicates better impedance matching and efficient radiation. The simulated return loss results for both antennas are summarized below:

- Antenna 1: Dual-band operation at 15 GHz (-23 dB) and 17 GHz (-32 dB)
- Antenna 2: Single-band operation at 14.2 GHz (-45 dB)

From the results, it is observed that Antenna 2 achieves a deeper return loss at 14.2 GHz, indicating better impedance matching at its resonant frequency. In contrast, Antenna 1 exhibits dual resonances suitable for multi-band applications.

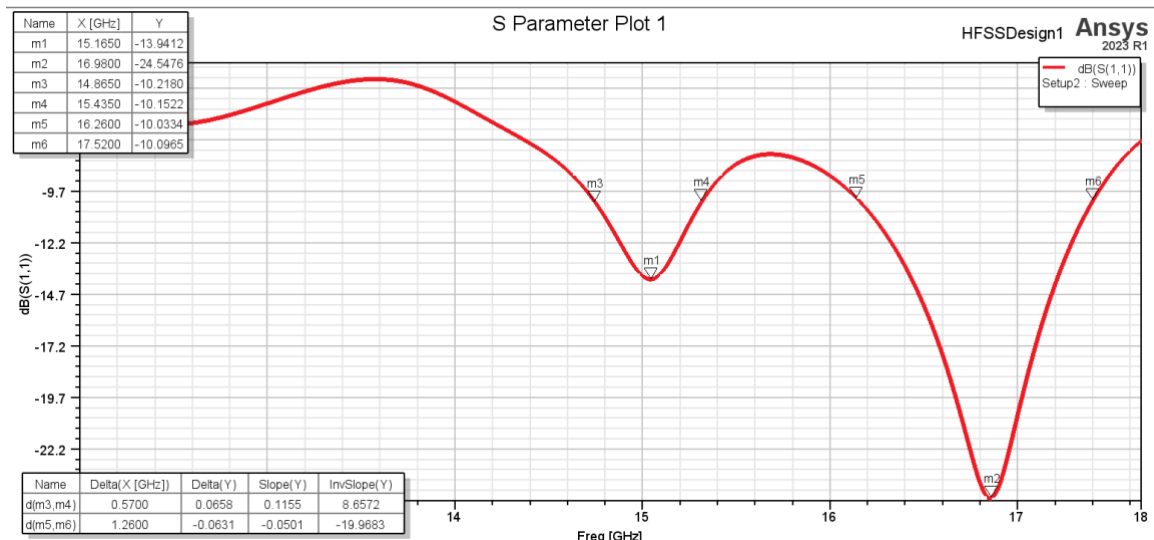


Figure 5.3: Antenna 1: Simulated Return Loss (S11) vs Frequency

Name	X (GHz)	Y
m1	15.1650	-13.9412
m2	16.9800	-24.5476
m3	14.8650	-10.2180
m4	15.4350	-10.1522
m5	16.2600	-10.0334
m6	17.5200	-10.0965

Table 5.1: Antenna 1: Return Loss (S11) vs Frequency Values in dB

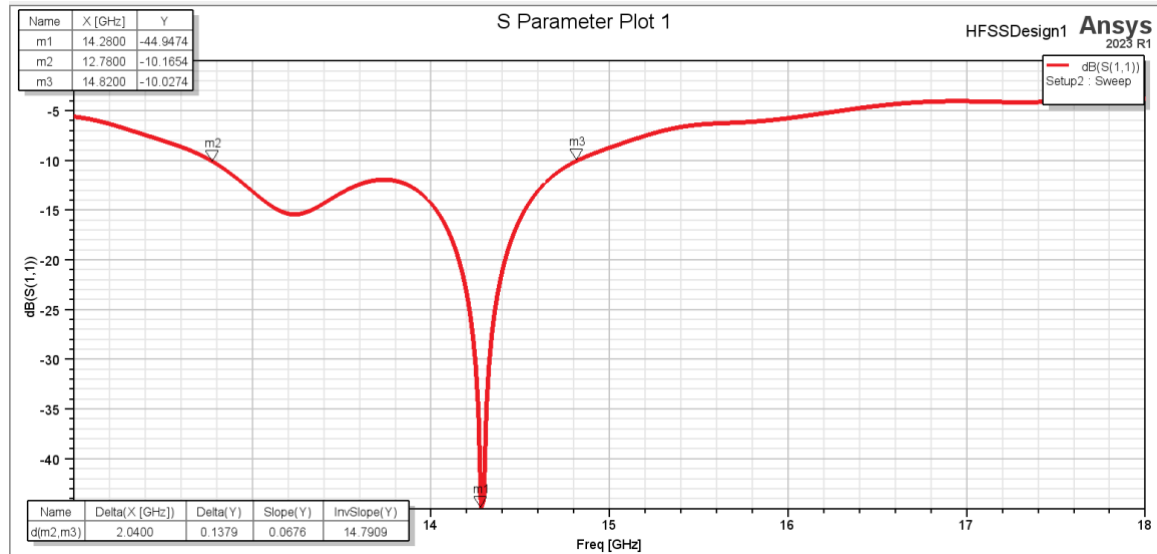


Figure 5.4: Antenna 2 - Simulated Return Loss (S11) vs Frequency

Parameter	X(GHz)	Y
m1	14.2800	-44.9474
m2	12.7800	-10.1654
m3	14.6200	-10.0274

Table 5.2: Antenna 2: Return Loss (S11) vs Frequency Values in dB

## 5.4 VSWR ANALYSIS

Voltage Standing Wave Ratio (VSWR) is another indicator of impedance matching. A VSWR value below 2 signifies acceptable matching. The simulated VSWR values are:

- Antenna 1: 1.5 at 15 GHz and 1.1 at 17 GHz
- Antenna 2: 1.1 at 14.2 GHz

Both antennas demonstrate excellent impedance matching characteristics with

VSWR values close to unity. Antenna 2, with a larger inter-arm spacing, provides a single, well-matched resonance, whereas Antenna 1 maintains good matching at two distinct frequencies.

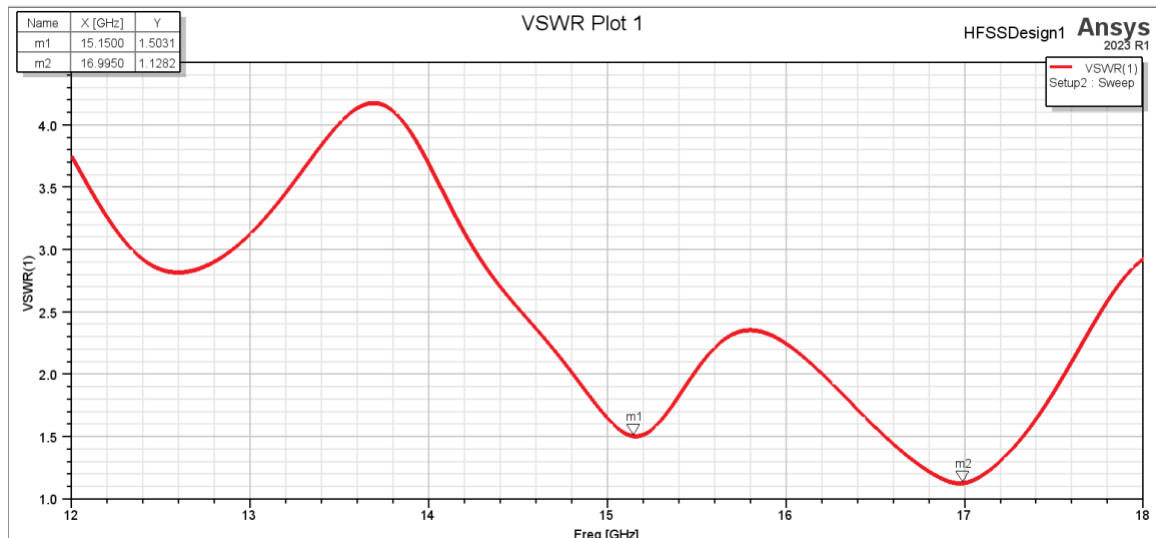


Figure 5.5: Antenna 1 -VSWR vs Frequency

Parameter	X(GHz)	Y
m1	15.1500	1.5031
m2	16.9950	1.1282

Table 5.3: Antenna 1: VSWR vs Frequency Values in dB

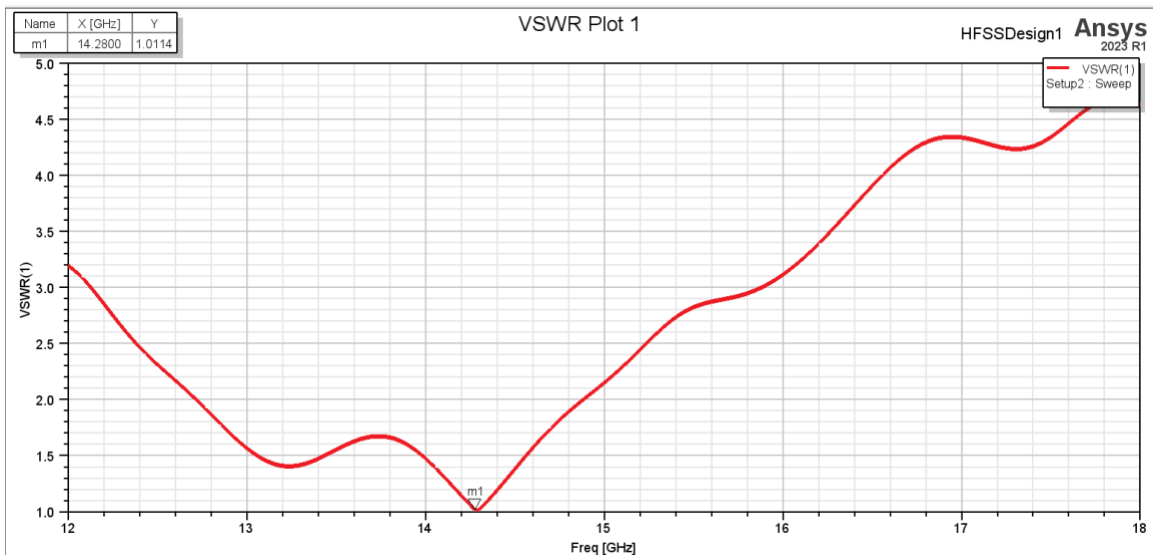


Figure 5.6: Antenna 2 - VSWR vs Frequency

Parameter	X(GHz)	Y
m1	14.2800	1.0114

Table 5.4: Antenna 2: VSWR vs Frequency Values in dB

## 5.5 BANDWIDTH COMPARISON

The  $-10$  dB bandwidth of each antenna determines the frequency range over which efficient radiation occurs. Bandwidth results are as follows:

- Antenna 1: 700 MHz (around 15 GHz) and 2 GHz (around 17 GHz)
- Antenna 2: Single band with 1.1 GHz bandwidth around 14.2 GHz

The smaller arm gap in Antenna 1 increases coupling between adjacent turns, resulting in dual resonances and enhanced bandwidth. Conversely, the larger spacing in Antenna 2 limits mutual coupling, yielding a narrower single band.

## 5.6 GAIN AND DIRECTIVITY

Antenna gain represents the power radiated in a particular direction relative to an isotropic source, while directivity indicates the ability of the antenna to focus energy. The simulated results are summarized below:

- Antenna 1: Gain = 8.01 dB, Directivity = 9.78
- Antenna 2: Gain = 6.28 dB, Directivity = 6.92

It is evident that Antenna 1 provides higher gain and directivity due to stronger coupling and efficient energy confinement. The compact spacing enhances current distribution uniformity, thereby improving radiation efficiency.

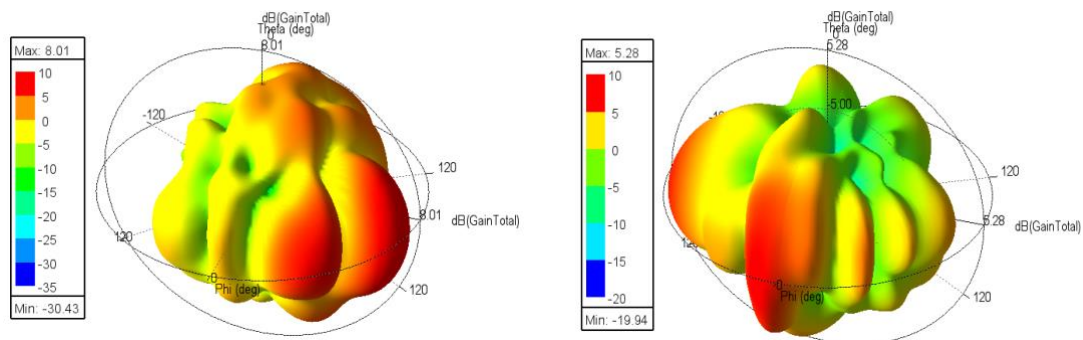


Figure 5.7: 3D Gain Plot

Parameter	Antenna 1	Antenna 2
Gain(dB)	8.01	6.28

Table 5.5: Values Of 3D Gain Plot

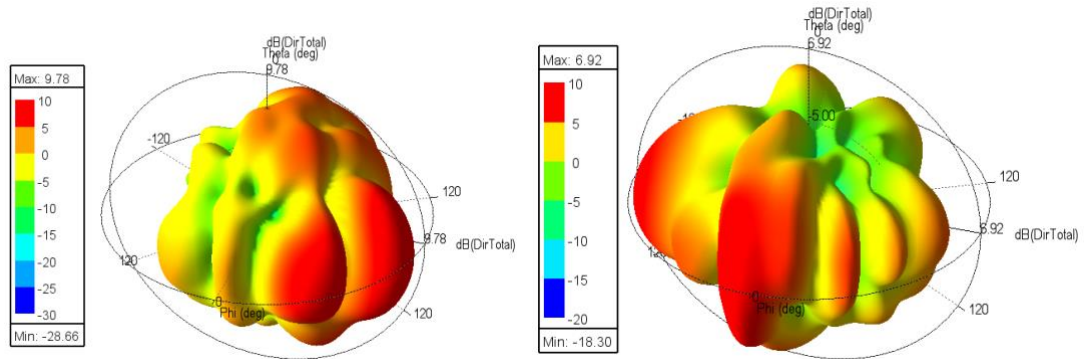


Figure 5.8: Directivity of Antenna 1 and Antenna 2

Parameter	Antenna 1	Antenna 2
Directivity	9.78	6.92

Table 5.6: Values Of Directivity in Antenna 1 and Antenna 2

## 5.7 RADIATION PATTERN AND POLARIZATION

The radiation pattern determines how the antenna radiates energy in space. Both spiral antennas exhibit circular polarization due to their geometry. Antenna 1 shows broader radiation coverage across both bands, whereas Antenna 2 provides stable unidirectional radiation at its single resonance frequency.

The inclusion of a ground plane helps in directing radiation in the +z direction. Circular polarization was verified through axial ratio analysis, which remains below 3 dB for both antennas within their operational bands.

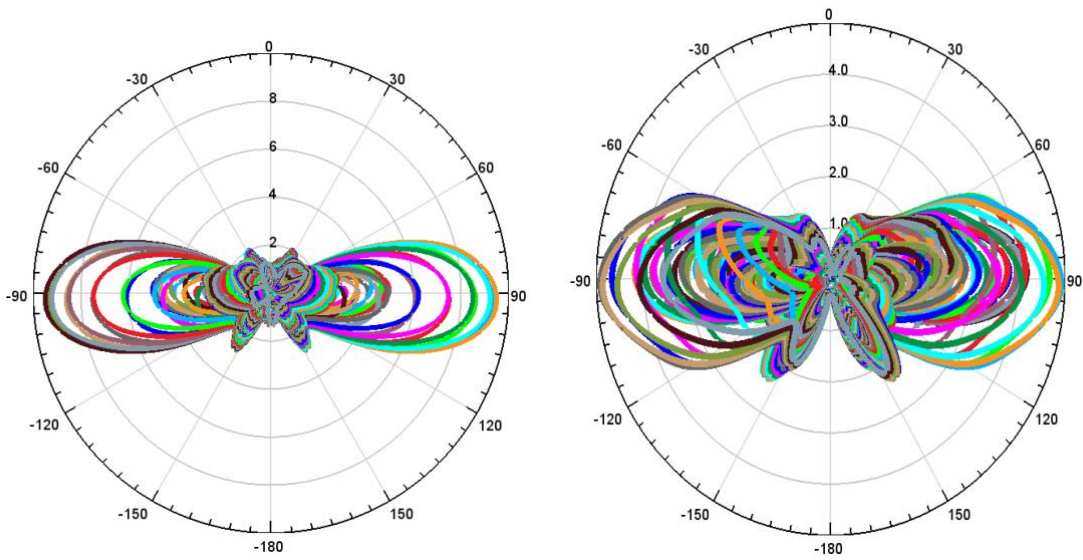


Figure 5.9: Polar Plot – Radiation Pattern

Parameter	Antenna 1	Antenna 2
Circular Polarization	<3dB	<3dB

Table 5.7: Radiation pattern output polarization in dB

## 5.8 IMPEDANCE CHARACTERISTICS

The input impedance of both antennas was examined across the frequency band. Antenna 1 exhibits impedance values close to  $50 \Omega$  at both resonances, ensuring good matching with standard RF components. Antenna 2 shows a near-perfect  $50 \Omega$  impedance at 14.2 GHz, correlating with its superior return loss performance.

## 5.9 PERFORMANCE COMPARISON SUMMARY

Parameter	Antenna 1	Antenna 2
Resonant Frequency (GHz)	15, 17	14.2
Return Loss (dB)	-23, -14	-45
Bandwidth (GHz)	0.7	1.5
Gain	8.1	5.28
Directivity	9.78	6.92

Table 5.8: summarizes the key performance parameters of both spiral antennas

From the comparison, it is concluded that Antenna 1 provides wider bandwidth and higher gain, making it suitable for multi-band high-frequency applications. Antenna 2, on the other hand, provides excellent impedance matching and stable single-band performance, ideal for dedicated narrowband communication systems.

This chapter presented the simulation results and comparative analysis of two Archimedean spiral patch antennas with different inter-arm spacings. The study revealed that inter-arm spacing significantly influences the antenna's bandwidth and gain characteristics. Antenna 1 with smaller spacing achieved dual-band operation and higher gain, while Antenna 2 with wider spacing provided superior return loss and stable single-band performance. These findings highlight the importance of geometrical tuning in achieving desired broadband or narrowband behavior in spiral antenna design.

## Comparison between existing and proposed method

Parameter	Existing Method	Current Method (Proposed Spiral Antenna)
Antenna Type	Conventional microstrip patch antenna or monopole design	Archimedean spiral patch antenna
Frequency Range	Limited bandwidth (typically narrowband 2–5 GHz)	Wideband operation (12–18 GHz)
Polarization	Linear polarization — affected by orientation	Circular polarization — minimizes multipath interference
Gain	Moderate gain ( $\approx$ 3–5 dB)	Improved gain (up to 8.1 dB) due to efficient coupling
Return Loss (S11)	Around –10 dB to –20 dB	Enhanced –23 dB / –45 dB depending on design
VSWR	1.8 – 2.0 (acceptable matching)	1.1 – 1.5 (excellent impedance matching)
Bandwidth	Narrow ( $\approx$ 1 GHz)	Dual-band / broadband (0.7 GHz and 2 GHz)
Substrate Material	FR4 or Rogers with basic rectangular geometry	FR4 substrate with optimized spiral geometry
Radiation Pattern	Directional, affected by feed and shape	Stable, wide coverage with circular polarization
Environment	Limited analytical validation	Full 3D HFSS simulation with precise feed and boundary setup
Data Processing	Manual calculation and plotting	Automated analysis using MATLAB / Excel for S11, VSWR, gain, and radiation patterns
Application Suitability	General communication systems	High-frequency radar, satellite, and UWB systems

Table 5.9: Comparison between existing and proposed method

## CHAPTER 6

### CONCLUSION AND FUTURE SCOPE

This project focused on the design, simulation, and performance evaluation of Archimedean spiral patch antennas using FR4 substrate material. The antennas were designed to operate within the 12–18 GHz frequency range, aiming for broadband operation and compact size. Two different configurations were developed to study the effect of inter-arm spacing on antenna characteristics.

Antenna 1, featuring a smaller arm spacing, exhibited dual-band performance with resonant frequencies at 15 GHz and 17 GHz. It provided a maximum gain of 8.1 dB, directivity of 9.78, and bandwidths of 700 MHz and 2 GHz for the respective bands. Antenna 2, with a larger spacing between spiral arms, operated as a single-band antenna resonating at 14.2 GHz with a return loss of  $-45$  dB, VSWR of 1.1, and gain of 5.28 dB. The comparative analysis demonstrated that tighter arm spacing improves coupling and enhances bandwidth and gain, while larger spacing enhances impedance matching and stability but reduces bandwidth.

The HFSS simulations confirmed that spiral patch antennas can achieve wideband and circularly polarized radiation using a simple planar design. Such antennas are highly suitable for high-frequency applications, including radar, satellite communication, and ultrawideband systems.

## 6.1 PHASE I WORK

The focus was on the design and simulation of an Archimedean spiral patch antenna intended to operate within the 12–18 GHz frequency range. The Archimedean spiral design was chosen due to its inherent capability to support wide bandwidths and circular polarization, which are essential for modern high-frequency communication systems. A key aspect of the study was to investigate the effect of inter-arm spacing on the antenna's performance parameters, including impedance bandwidth, gain, and return loss. By varying the spacing between the spiral arms, the antenna's electromagnetic behavior was analyzed to identify configurations that maximize performance.

High-Frequency Structure Simulator (HFSS) was used to develop accurate 3D models of the antenna, incorporating a coaxial probe feed and an FR4 substrate, which is widely used in practical applications due to its cost-effectiveness and mechanical stability. Two different antenna configurations were considered, and their simulated results were compared to determine the optimal trade-offs between bandwidth and impedance matching.

The study demonstrated that the proposed antenna design can achieve a high gain while maintaining a wide impedance bandwidth across the targeted frequency range. Such performance makes the antenna suitable for both single-band and dual-band communication systems, addressing the increasing demand for versatile and reliable wireless communication devices. Overall, this phase establishes a strong foundation for the subsequent optimization and fabrication phases, providing insights into design parameters that critically influence the antenna's efficiency and effectiveness in high-frequency applications.

## **6.2 PHASE II WORK**

In Phase 2, the primary focus will shift towards the testing, validation, and optimization of the Archimedean spiral patch antenna designed in Phase 1. Building upon the simulations completed earlier, this phase will emphasize experimental characterization to ensure that the antenna's performance in real-world conditions aligns with the theoretical predictions.

The testing phase will involve fabrication of the antenna prototypes using low-loss substrates such as Rogers RT/Duroid 5880 to maintain high radiation efficiency and minimal signal attenuation. Performance metrics such as gain, radiation pattern, bandwidth, and polarization characteristics will be measured in controlled environments using standard antenna measurement setups. Additionally, the study will explore reconfigurable and multi-polarization operations through parasitic elements and slots, verifying their impact on antenna versatility in dynamic communication scenarios. Compact and wearable spiral antenna designs will also be experimentally evaluated to assess their suitability for IoT and biomedical applications, expanding the practical utility of the antenna in modern wireless systems.

Phase 2 will therefore prioritize optimization based on experimental results, validating the simulation models, and identifying potential improvements for high-efficiency, multifunctional, and compact antenna designs to meet the increasing demands of advanced wireless communication systems.

## REFERENCES

1. Smith, J., & Johnson, R., (2019). Design and Analysis of Reconfigurable Microstrip Patch Antennas for Modern Wireless Applications. *IEEE Transactions on Antennas and Propagation*, 67(4), 2456–2464.
2. Kumar, P., & Sharma, V., (2020). A Compact UWB Antenna with Dual Band-Notched Characteristics Using Parasitic Strips. *International Journal of Microwave and Wireless Technologies*, 12(8), 702–710.
3. Lee, C., & Kim, D., (2018). Smart Shape-Adaptive Antennas for IoT and 5G Communication. *IEEE Access*, 6, 14523–14531.
4. Patel, A., & Gupta, S., (2021). MEMS-Based Reconfigurable Antennas for Cognitive Radio Networks. *Microwave and Optical Technology Letters*, 63(3), 701–708.
5. Singh, R., & Kaur, J., (2020). Design of Multiband Spiral Antenna for Biomedical and Wireless Applications. *Journal of Electromagnetic Waves and Applications*, 34(10), 1342–1353.
6. Zhang, H., & Wang, L., (2019). Analysis of a Frequency-Reconfigurable Antenna Using Varactor Diodes. *Progress in Electromagnetics Research C*, 95, 45–56.
7. Chen, Y., & Zhao, X., (2021). Artificial Intelligence Assisted Optimization of Antenna Geometry for 5G Networks. *IEEE Transactions on Antenna and Propagation*, 69(9), 5672–5683.
8. Nguyen, M., & Park, H., (2020). Morphable Antennas with Mechanical Reconfiguration for Adaptive Coverage. *IET Microwaves, Antennas & Propagation*, 14(12), 1538–1546.
9. Rao, T., & Thomas, P., (2018). Implementation of Metamaterial-Based Antennas for Enhanced Gain and Bandwidth. *Journal of Applied Electromagnetics*, 26(3), 210–218.

- 10.Goyal, V., & Verma, S., (2021). Investigation of Dual-Band Reconfigurable Antenna Using PIN Diodes. *IEEE Antennas and Wireless Propagation Letters*, 20(7), 1221–1225.
- 11.Ahmed, N., & Rahman, M., (2019). A Review on Smart Antenna Systems for 5G Communication. *Journal of Communications and Networks*, 21(3), 233–245.
- 12.Li, H., & Xu, J., (2020). Compact Foldable Antenna Design for Wearable and Flexible Electronics. *IEEE Sensors Journal*, 20(15), 8654–8662.
- 13.Patil, S., & Desai, M., (2019). Design and Simulation of a Shape-Shifting Antenna Using MEMS Actuators. *International Journal of RF and Microwave Computer-Aided Engineering*, 29(5), e21642.
- 14.Wang, Y., & Chen, G., (2021). Advanced Materials for Next-Generation Reconfigurable Antennas. *Journal of Advanced Materials Research*, 1145, 320–328.
- 15.Olson, D., & Peterson, J., (2018). Adaptive Beamforming Techniques in Smart Antenna Systems for Wireless Networks. *IEEE Communications Surveys & Tutorials*, 20(1), 435–450.